Developmental Cell
Article

HTP-3 Links DSB Formation with Homolog Pairing and Crossing Over during *C. elegans* Meiosis

William Goodyer,[1] Susanne Kaitna,[1] Florence Couteau,[1] Jordan D. Ward,[2] Simon J. Boulton,[2] and Monique Zetka[1,*]
[1]Department of Biology, McGill University, Montreal, Quebec H3A 1B1, Canada
[2]DNA Damage Response Laboratory, Cancer Research UK, London Research Institute, Clare Hall Laboratories, South Mimms EN6 3LD, United Kingdom
*Correspondence: monique.zetka@mcgill.ca
DOI 10.1016/j.devcel.2007.11.016

SUMMARY

Repair of the programmed meiotic double-strand breaks (DSBs) that initiate recombination must be coordinated with homolog pairing to generate crossovers capable of directing chromosome segregation. Chromosome pairing and synapsis proceed independently of recombination in worms and flies, suggesting a paradoxical lack of coregulation. Here, we find that the meiotic axis component HTP-3 links DSB formation with homolog pairing and synapsis. HTP-3 forms complexes with the DSB repair components MRE-11/RAD-50 and the meiosis-specific axis component HIM-3. Loss of *htp-3* or *mre-11* recapitulates meiotic phenotypes consistent with a failure to generate DSBs, suggesting that HTP-3 associates with MRE-11/RAD-50 in a complex required for meiotic DSB formation. Loss of HTP-3 eliminates HIM-3 localization to axes and HIM-3-dependent homolog alignment, synapsis, and crossing over. Our study reveals a mechanism for coupling meiotic DSB formation with homolog pairing through the essential participation of an axis component with complexes mediating both processes.

INTRODUCTION

In the vast majority of sexually reproducing organisms, the segregation of chromosomes at the first meiotic division relies on the maturation of recombination events into the crossovers capable of biorienting the kinetochores to opposite poles. Most, if not all, meiotic recombination initiates with the formation of programmed double-strand breaks (DSBs) catalyzed by Spo11p, an evolutionarily conserved type II topoisomerase-like transesterase. While the events and preconditions leading to Spo11p-mediated meiotic DSB formation are poorly understood, meiotic DSB formation is regulated at the level of chromatin accessibility (Murakami et al., 2003; Reddy and Villeneuve, 2004) by the activity of other proteins required for DSB formation and by Cdk activity (Henderson et al., 2006). In *S. cerevisiae*, for example, the Mre-11-Rad50-Xrs2 (MRX) complex and at least six other genes are required for DSB formation (reviewed by Keeney, 2001). Once initiated, the conserved DSB-generating reaction yields Spo11p covalently associated with the free 5′ strand termini, and the repair of the DSB requires the release of Spo11p through an asymmetrical endonucleolytic cleavage activity that is thought to originate in the MRX complex of yeast and the analogous Mre11-Rad50-Nbs1 (MRN) complex in vertebrates (Neale et al., 2005). This resection generates 3′ ssDNA overhangs which are bound by members of the bacterial RecA family of strand-exchange proteins (Rad51, Dmc1) and which initiate a search for homology that culminates in the repair of the DSB (reviewed by Neale and Keeney, 2006). Since only recombination intermediates that use the homolog as a repair template can generate the crossover critical for meiotic segregation, recombination must be coupled to homologous chromosome pairing to ensure the spatial availability of the chiasma-generating template.

Meiotic chromosome pairing consists of at least three successive steps: a long-range interaction which facilitates homolog recognition, the alignment of identical chromosome pairs along their lengths at a distance (also known as homolog juxtaposition or presynaptic alignment), and an intimate association of aligned homologs at a distance of 100 nm through synapsis (Zickler, 2006). These events are combined with dramatic changes in chromosome morphology: first, the assembly of a proteinaceous axial element between newly replicated sister chromatids, and second, the polymerization of transverse filament proteins between the axes of homologous chromosomes, giving rise to the tripartite proteinaceous structure that defines synapsis, the synaptonemal complex (SC) (Kleckner, 2006). While studies from plant, animal, and fungal model systems collectively seem to suggest that the process of homolog recognition is independent of the recombination pathway, different organisms show different dependencies on meiotic DSB formation and recombination initiation in achieving presynaptic alignment and synapsis. At one end of the spectrum, wild-type levels of DSB formation are required to form recombination-based connections between homologous chromosome axes to align them (Tessé et al., 2003; Peoples et al., 2002), followed by the initiation of synapsis at the sites of a subset of axial associations destined to become crossovers (Henderson and Keeney, 2005). Consequently, the recombination pathway is functionally interdigitated with presynaptic alignment and synapsis; meiotic DSB formation and recombination are required for presynaptic alignment and the initiation of synapsis, and SC formation is required for the maturation of axial associations into crossovers. In contrast, homolog recognition, presynaptic alignment, and synapsis proceed in the absence of DSBs and recombination in *C. elegans* and *Drosophila*, culminating in homologously synapsed chromosome pairs (Dernburg et al., 1998; McKim et al., 1998). Furthermore,

recombination is initiated at wild-type levels in nematode mutants in which chromosomes fail to align and synapse (Couteau et al., 2004), indicating that homolog alignment and synapsis are not a prerequisite for DSB formation and repair. Despite this seeming lack of mechanistic coupling between the recombination and chromosome-pairing pathways, the processing of recombination intermediates into crossovers strictly depends on the assembly of the SC between homologous chromosome axes (MacQueen et al., 2002; Colaiácovo et al., 2003), indicating that recombination and chromosome "pairing" must be coordinated during wild-type meiosis to achieve crossover formation.

Although the precise mechanism is unknown, chromosome morphogenesis, and in particular chromosome axes, has been extensively implicated as an evolutionarily conserved conduit for coordinating recombination initiation and progression with chromosome pairing status during meiosis. In *S. cerevisiae*, axis components such as Hop1p and Red1p are required to establish normal levels of meiotic DSBs in addition to their essential function in synapsis, revealing a role for structural components in localization or activation of Spo11p. This is a functionally economical scenario in the case of Hop1, since it is also required to establish the barrier to using the sister chromatid as a repair template and for SC assembly, thereby promoting repair of the recombination intermediate using the homolog as a partner and generating the chiasmata critical for proper chromosome segregation at meiosis (Niu et al., 2005). In *C. elegans*, the proper execution of homolog pairing, synapsis, and crossing over depends on the activity of the meiosis-specific axis component HIM-3 and its three paralogs (Zetka et al., 1999; Couteau et al., 2004; Couteau and Zetka, 2005; Martinez-Perez and Villeneuve, 2005; this study). HIM-3 is essential for homolog alignment and synapsis, and functions in the barrier-to-sister chromatid exchange (BSCE) during recombination (Zetka et al., 1999; Couteau et al., 2004). In this study, we find that the HIM-3 paralog HTP-3 is a germline-specific protein that associates with chromatin in premeiotic nuclei and is a component of meiotic chromosome axes. While the other members of the HIM-3 family are dispensable for recombination initiation, our results suggest that HTP-3 forms complexes with MRE-11/RAD-50 to mediate meiotic DSB formation and with HIM-3 to mediate homolog alignment and synapsis, revealing HTP-3 to be critical for the processes of recombination initiation, homolog alignment, and synapsis.

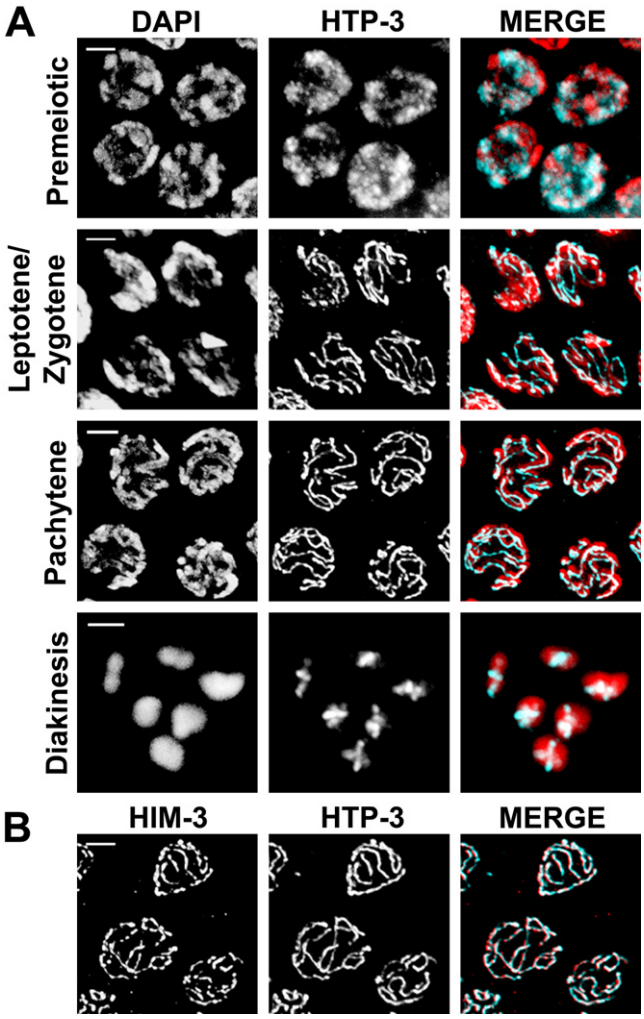

Figure 1. HTP-3 Localizes to Germline Nuclei and Colocalizes with HIM-3 to Meiotic Chromosome Cores

High-magnification immunofluorescence micrographs of HTP-3 localization during meiotic prophase in wild-type germlines (A). In premeiotic nuclei, HTP-3 (cyan) is largely colocalized with the DAPI-stained chromatin (red). In early prophase nuclei at the leptotene-zygotene stage, HTP-3 localizes to assembling meiotic chromosome axes. At mid-pachytene, HTP-3 is localized to synapsed chromosome axes. Following desynapsis, HTP-3 localization adopts a cruciform pattern on the condensed bivalents of diakinesis nuclei. (B) Anti-HTP-3 and anti-HIM-3 signals colocalize along the lengths of synapsed chromosomes in pachytene nuclei. Scale bars, 3 μM.

RESULTS

HTP-3 Localizes to Chromatin Premeiotically and Is a Component of Meiotic Chromsome Axes

The germline of *C. elegans* is a syncytium of nuclei representing a spatio-temporal progression through meiotic prophase that is easily observed in three-dimensionally preserved DAPI-stained germlines. Upon entering the meiotic cell cycle, nuclei enter the transition zone (corresponding to leptotene-zygotene; Dernburg et al., 1998) and are cytologically distinguishable by their crescent-shaped appearance, a consequence of the chromosome clustering that is associated with this stage. Nuclei then enter the pachytene region of the germline where the fully aligned and synapsed homologs are evident as equidistantly spaced, parallel tracks; following desynapsis at diplotene, the chiasmata joining chromosome pairs are revealed. To investigate the localization of HTP-3, polyclonal antibodies were raised against the C-terminal portion of the protein (aa 414–607); HTP-3 localized to all nuclei within the germline, both those proliferating mitotically and those engaged in the meiotic cell cycle (Figure 1A). In premeiotic nuclei, HTP-3 staining assumed a diffuse pattern that overlapped the DAPI-stained chromatin in interphase nuclei (Figure 1A) but was not detectable on the condensed chromatin of M-phase nuclei (data not shown). Upon entry into meiotic prophase, HTP-3 localized to chromosome axes, consistent with a previous report (MacQueen et al., 2005), and colocalized with HIM-3 throughout meiotic prophase (Figure 1B and data not shown).

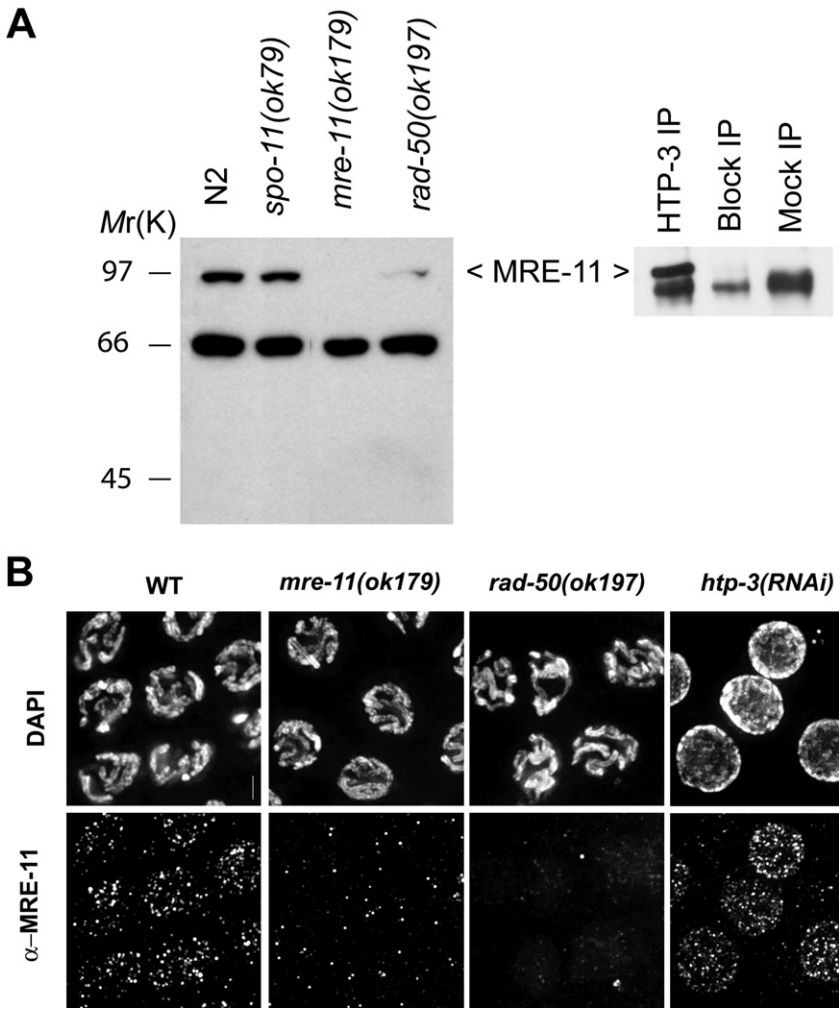

Figure 2. HTP-3 Associates with MRE-11 in a Complex In Vivo

(A) Western blot analyses using extracts derived from 50 adult hermaphrodites of the indicated genotype probed with anti-MRE-11 antibody. Wild-type levels of MRE-11 are detected in *spo-11* mutants, but no protein is detectable in *mre-11* deletion mutants and decreased levels are detected in *rad-50* mutants. Western blot of immunoprecipitations from staged adult hermaphrodite extracts using anti-MRE11 antibodies. MRE-11 is not detected in IPs first blocked with HTP-3 antigen (Block-IP) or in mock reactions containing anti-HTP-3 and IP buffer alone (Mock-IP).

(B) High-magnification immunofluoresence micrographs of mid-pachytene nuclei from germlines of the indicated genotype stained with anti-MRE-11. MRE-11 is detected as foci in WT and *htp-3 (RNAi)* germlines, whereas only background levels can be detected in *mre-11* and *rad-50* mutants. Scale bars, 2 μm.

HTP-3 Forms Complexes In Vivo with MRE-11/RAD-50 and HIM-3

The localization of HTP-3 to both premeiotic chromatin and to meiotic chromosome axes suggested that the protein associated with distinct complexes, and we next used a biochemical approach to reveal its potential functions by identifying the components in HTP-3-containing complexes. Unique protein bands from HTP-3 immunoprecipitates were identified and analyzed by mass spectroscopy (data not shown). As expected, HTP-3 was among the bands at relative molecular mass 66,000 (Mr 66K). In addition, a significant number of peptide fragments matched the tryptic peptides predicted for the worm homologs of two components of the yeast MRX complex, MRE-11 and RAD-50, and for the HTP-3 paralog HIM-3. However, no interacting candidates corresponded to the putative *C. elegans* Xrs2 homolog, XNP-1 (Garcia-Muse and Boulton, 2007). To confirm the interaction with MRE-11, we raised anti-MRE-11 antibodies (Experimental Procedures) and identified MRE-11 in western blot analyses of HTP-3-immunoprecipitated complexes derived from adult stage hermaphrodite extracts, but not in control reactions (Figure 2A). Immunolocalization of MRE-11 in *mre-11(ok179)* deletion mutants detected only nonspecific background staining, consistent with the lack of detectable MRE-11 in western blot analyses of mutant germlines (Figures 2A and 2B). Since no mutants of *htp-3* exist, we used RNA interference (RNAi) to investigate the role of the gene during meiosis (Experimental Procedures). In wild-type, *htp-3(RNAi)*, and *spo-11(ok79)* germlines, MRE-11 staining was evident as abundant nuclear foci throughout meiosis (Figure 2B and data not shown), indicating that bulk MRE-11 stability and localization was not dependent on the presence of HTP-3, SPO-11, or meiotic DSBs per se. In contrast, in *rad-50(ok197)* mutants little MRE-11 was detected in western blot analyses, and levels similar to those observed for *mre-11* mutants were detected by immunostaining of *rad-50* mutant germlines (Figure 2), suggesting that MRE-11 is unstable unless associated with RAD-50.

To confirm that HTP-3 and HIM-3 form a complex in vivo, we immunoprecipitated HTP-3-containing complexes and probed for the presence of HIM-3 on western blots (Figure 3A). Anti-HTP-3 antibodies immunoprecipitated HIM-3 from staged adult hermaphrodite extracts; specificity of the interaction is demonstrated by the failure to detect HIM-3 in western blots of a mock immunoprecipitation reaction and by the loss of the interaction in immunoprecipitation reactions in which the antibody was first blocked with the HTP-3 antigen. To functionally investigate this biochemical interaction, we examined HTP-3 localization in *him-3(gk149)* null mutant germlines and HIM-3 localization in *htp-3(RNAi)* germlines. While HTP-3 localized to chromosome axes in *him-3* null mutants at appropriate levels and with normal timing, no HIM-3 could be detected at chromosome axes of *htp-3(RNAi)* meiotic nuclei at any stage, indicating that HTP-3 recruitment to meiotic chromosome axes is a prerequisite for subsequent HIM-3 association (Figures 3B and 3C; data not shown). Surprisingly, little HIM-3 was detectable in *htp-3(RNAi)* nuclei per se, despite the fact that the *him-3* transcript could

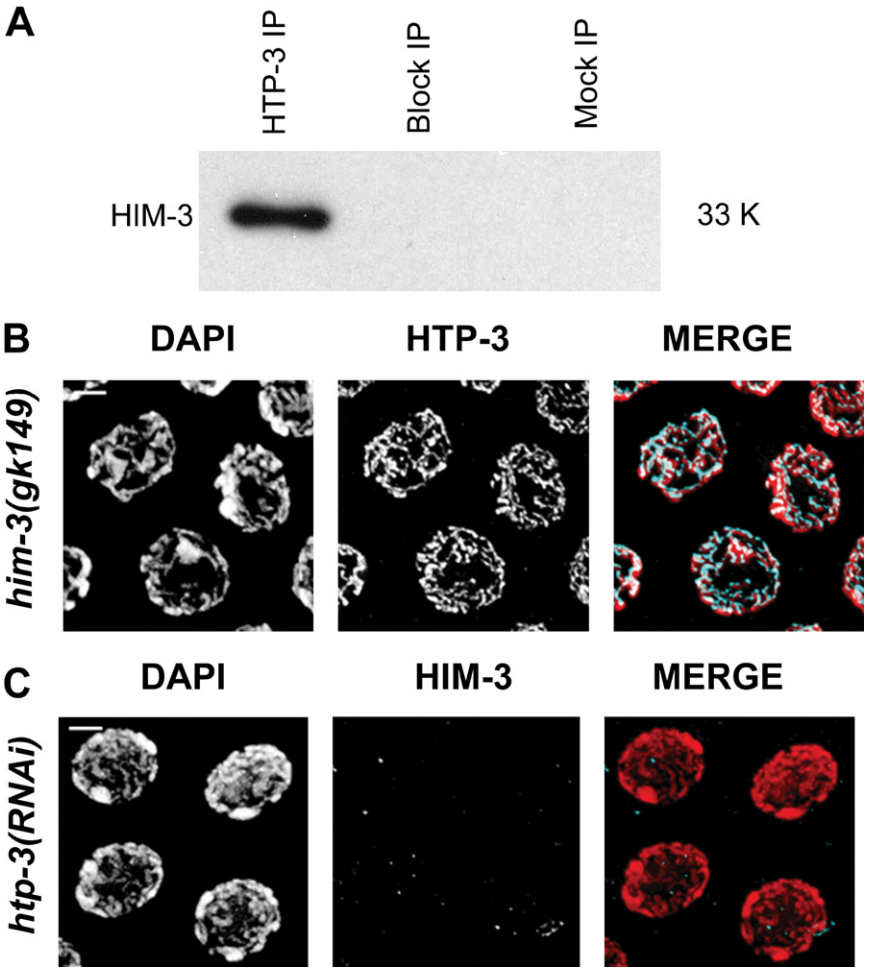

Figure 3. HTP-3 Forms a Complex with HIM-3 In Vivo and Is Required for HIM-3 Localization

(A) Western blot analysis of HTP-3 immunoprecipitates (IP) with anti-HIM-3 antibodies reveals the presence of HIM-3. HIM-3 is not detected in control IPs using either HTP-3 antibody blocked by preincubation with HTP-3 antigen (block IP) or in mock IP reactions (HTP-3 antibody in IP buffer).

(B and C) High-magnification immunofluorescence micrographs of *him-3(gk149)* and *htp-3(RNAi)* mutant nuclei from the pachytene region of the germlines (zone IV). (B) HTP-3 localizes to unsynapsed axes in *him-3(gk149)*. (C) HIM-3 fails to localize to chromosome axes in *htp-3(RNAi)* germlines. Scale bars, 2 μm.

be detected by RT-PCR in *htp-3(RNAi)* germlines (see Figure S1 in the Supplemental Data available with this article online), suggesting that HIM-3 may be unstable or undetectable when not axis associated. Taken together, the pattern of HTP-3 localization and our biochemical results suggest that HTP-3 associates with distinct complexes to function at two interfaces: the MRE-11/RAD-50 complex at the chromatin interface and with HIM-3 at the chromosome axis interface.

RAD-51- and RPA-1-Marked Early Recombination Intermediates Fail to Form in *htp-3(RNAi)*

We next investigated the functional significance of the HTP-3/MRE-11 interaction. In *S. cerevisiae*, Mre11p is required for DSB formation and processing, and several lines of evidence suggest a similar role for the worm homolog. In wild-type *C. elegans* meiosis, chiasmata physically link each pair of the six chromosomes, which resolve into six DAPI-stained bodies, or bivalents, in ooctye nuclei at the final stage of meiotic prophase, known as diakinesis. *mre-11* mutants predictably fail to make chiasmata, and instead 12 well-formed univalents are evident at diakinesis (Chin and Villeneuve, 2001), identical to those observed in *spo-11* mutants (Dernburg et al., 1998). Furthermore, they do not show the chromatin decondensation defect of DSB repair mutants that originates with the presence of unrepaired meiotic DSBs (Alpi et al., 2003; Martin et al., 2005), and instead *mre-11(RNAi)* rescues the DSB-dependent decondensation defect of diakinesis chromosomes of *rad-51* mutants (Figure 4C), suggesting the nematode MRE-11 has a conserved role in meiotic DSB formation. Given that HIM-3 is dispensable for recombination initiation (Couteau et al., 2004), we sought to investigate if the role of HTP-3 in HTP-3/MRE-11 complexes could be at the level of DSB formation.

To examine the role of HTP-3 in recombination initiation, we used an antibody to RAD-51—a protein involved in the strand-exchange steps of DSB repair during HR and whose localization is dependent on the presence of DSBs (Colaiácovo et al., 2003)—to monitor early recombination events (Figures 4A and 4B). In a time course analysis of RAD-51 foci appearance and disappearance in wild-type and *him-3* null mutant germlines, the number of RAD-51-marked nuclei and the number of RAD-51 foci per nucleus peak in early pachytene (zone III) (Colaiácovo et al., 2003; Couteau et al., 2004). Surprisingly, we could detect only background levels of RAD-51 foci throughout *htp-3(RNAi)* germlines (data not shown), and in zone III, the level of detectable RAD-51 foci was not statistically different from *spo-11(ok79)* null mutants (Figure 4A), in which DSBs fail to form (Dernburg et al., 1998), despite the fact *spo-11* transcripts could be detected by RT-PCR (Figure S1), indicating the gene was expressed. Since γ-irradiation-induced DSBs can bypass the need for SPO-11 activity in recombination initiation in *C. elegans* (Dernburg et al., 1998; Kelly et al., 2000), RAD-51 localization was examined in irradiated *htp-3(RNAi)* germlines to determine if the lack of RAD-51 foci was a failure in the expression of RAD-51 or its localization to DSBs. RAD-51 localized to chromosomes in both *htp-3(RNAi)*- and control *spo-11(ok79)*-irradiated germlines, indicating that the protein was both expressed and competent to localize to artificially provided DSBs in the absence of HTP-3 (Figure 4B). Furthermore, 12 well-formed univalents were observed in *htp-3(RNAi)* germlines following irradiation (Figure 4C), indicating that DSBs can be efficiently repaired in the absence of HTP-3. Similar to the RAD-51-marked recombination intermediates

that form in synapsis-defective mutants (Colaiácovo et al., 2003) and in *him-3* null mutants (Couteau et al., 2004), these artificially provided DSBs are likely to be repaired using the sister chromatid as a repair template, since sister chromatid cohesion is required for meiotic DSB repair (Pasierbek et al., 2001, 2003; Wang et al., 2003) and mutants in components of the homologous recombination (HR) repair pathway exhibit chromosome fragmentation at diakinesis in the presence of DSBs (Chin and Villeneuve, 2001; Alpi et al., 2003; Martin et al., 2005). To determine if early recombination intermediates not yet processed for RAD-51 loading form in *htp-3(RNAi)* germlines, we next examined the localization of RPA-1, the *C. elegans* homolog of replication protein A that rapidly binds the ssDNA tail generated during HR before being displaced by RAD-51. Several aspects of RAD-51 activity, including the displacement of RPA-1, are regulated by BRC-2, the homolog of the human DNA repair gene BRCA2. In *C. elegans brc-2(tm1086)* mutants, RPA-1 foci accumulate and persist at inappropriately late stages of meiosis in a DSB-dependent manner compared to wild-type (Martin et al., 2005). While a similar accumulation of RPA-1-marked foci was observed in the late-pachytene nuclei of *brc-2* mutants, no foci were detected in nuclei of that stage in *htp-3(RNAi)* germlines (Figure S2), corroborating the interpretation that the resected meiotic DSBs central to the HR mechanism did not form in the absence of HTP-3.

htp-3(RNAi) Rescues the DSB-Dependent Diakinesis Defects of *rad-51* and *brc-2* Mutants

Given our inability to detect the earliest intermediates of HR-mediated DSB repair, we next considered the possibility that HTP-3 is required for the formation of meiotically programmed DSBs by investigating if *htp-3(RNAi)* could rescue the DSB-dependent defects of HR-defective mutants (Rinaldo et al., 2002; Takanami et al., 2003; Alpi et al., 2003; Martin et al., 2005). In the absence of RAD-51 or BRC-2, homologs align and synapse; however, at diakinesis the chromosomes appear as decondensed and aggregated masses, a *spo-11*-dependent phenotype thought to be due to the accumulation of unrepaired meiotic DSBs (Alpi et al., 2003). In the diakinesis nuclei of *rad-51(lg8701); htp-3(RNAi)* and *brc-2(tm1086); htp-3(RNAi)* germlines, 12 well-condensed univalents were formed (Figure 4C), similar to those observed at diakinesis in *rad-51(RNAi); spo-11(ok79)* and *brc-2(tm1086); spo-11(ok79)* double mutants in which DSBs fail to form (Rinaldo et al., 2002; Takanami et al., 2003; Martin et al., 2005).

htp-3(RNAi) Does Not Activate RAD-51-Independent Repair Pathways in the Germline

In principle, germline DSBs (both artificially induced and *spo-11* catalyzed) could potentially be repaired by the nonhomologous end-joining pathway (NHEJ). While the HR pathway uses homologous sequences on the sister chromatid or homolog as a template for error-free repair, the NHEJ pathway results in the direct ligation of broken DNA ends via an error-prone mechanism that can generate mutations. Likely as a consequence of the potential for genome instability through NHEJ-mediated DSB repair and the inability of this pathway to generate chiasmata, *C. elegans* uses HR to repair both radiation-induced and meiotically programmed DSBs in germ cells at all times (Clejan et al., 2006), despite the fact that genes encoding the core NHEJ factors *lig-4*, *cku-70*, and *cku-80* are expressed at high levels in the germline (Reinke et al., 2004). Since NHEJ components are potentially functional in the germline, we investigated if meiotic DSBs were inappropriately repaired using NHEJ in the absence of HTP-3, thereby excluding the formation of RAD-51-marked intermediates. Mutants in *C. elegans lig-4*, the ligase catalyzing the sealing of DSBs during the repair reaction, show no defects in meiotic processes, and prophase nuclei arrive at diakinesis with the six bivalents observed in wild-type germlines (Martin et al., 2005, this study); however, *rad-51(RNAi)* in *lig-4* mutants results in the chromatin decondensation and chromosome aggregation typical of *rad-51* mutants, consistent with the primacy of HR-mediated repair of meiotic DSBs (Figure 4C). The rescue of the diakinesis defects observed in *rad-51; htp-3(RNAi)* germlines cannot be explained by inappropriate activation of the NHEJ pathway since 12 well-formed univalents are consistently observed in the diakinesis nuclei of *lig-4; rad-51(RNAi); htp-3(RNAi)* in which the NHEJ pathway is inactive. Taken together, our results demonstrate a NHEJ-independent rescue of DSB-dependent defects of HR mutants in the absence of HTP-3 that is most parsimoniously explained by an essential function for HTP-3 during meiotic DSB formation per se.

Analysis of the chromatin-associated protein HIM-17 suggested the involvement of histone modifications in rendering chromatin competent for meiotically programmed DSBs (Reddy and Villeneuve, 2004). Given that the absence of HTP-3 does not detectably affect HIM-17 localization (data not shown) or result in the Him-17-related deficits in H3MeK9 levels that are correlated with the loss of competency to form meiotic DSBs (Figure S3), the requirement for HTP-3 in DSB formation defines a new mechanism of regulation.

Recombination Initiation in *scc-3* Mutants Is HTP-3 Dependent

The association of HTP-3 to chromatin in premeiotic germline nuclei and to meiotic chromosome is similar to the localization observed for cohesins, the multisubunit complex that mediates sister chromatid cohesion during mitosis and meiosis (Pasierbek et al., 2001, 2003; Chan et al., 2003). The cohesin complex is composed of four conserved proteins: the two SMC (structural maintenance of chromosomes) SMC-1 and SMC-3 encircle the sister chromatids and form a ring in conjunction with two non-SMC components, SCC-3 and SCC-1 (or its meiotic counterpart REC-8) (reviewed by Nasmyth and Haering, 2005). In *C. elegans*, sister chromatid cohesion has been shown to be required for the formation of meiotic chromosome axes since in both *rec-8* and *scc-3* mutants, the axis component HIM-3 fails to localize (Pasierbek et al., 2001, 2003). Similarly, in *scc-3*-depleted germlines in which REC-8 fails to load and sister chromatid cohesion is severely abrogated (Wang et al., 2003; Pasierbek et al., 2003), HTP-3 was mislocalized (Figure 5A). In premeiotic nuclei, HTP-3 localization was disrupted, although some HTP-3 still detectably colocalized with chromatin. In meiotic nuclei, HTP-3 localized to one or a few aggregates within the nucleoplasm from the earliest stages of meiotic prophase entry (Figure 5A and data not shown), a pattern reminiscent of HIM-3 mislocalization reported in *scc-3(RNAi)* (Pasierbek et al., 2003). From these results, we conclude that cohesins provide a structural platform for the recruitment of HTP-3 and downstream axis components like HIM-3.

In budding yeast, the detection of DSB formation in chromatin loops, rather than in axis-associated DNA sequences, has led to

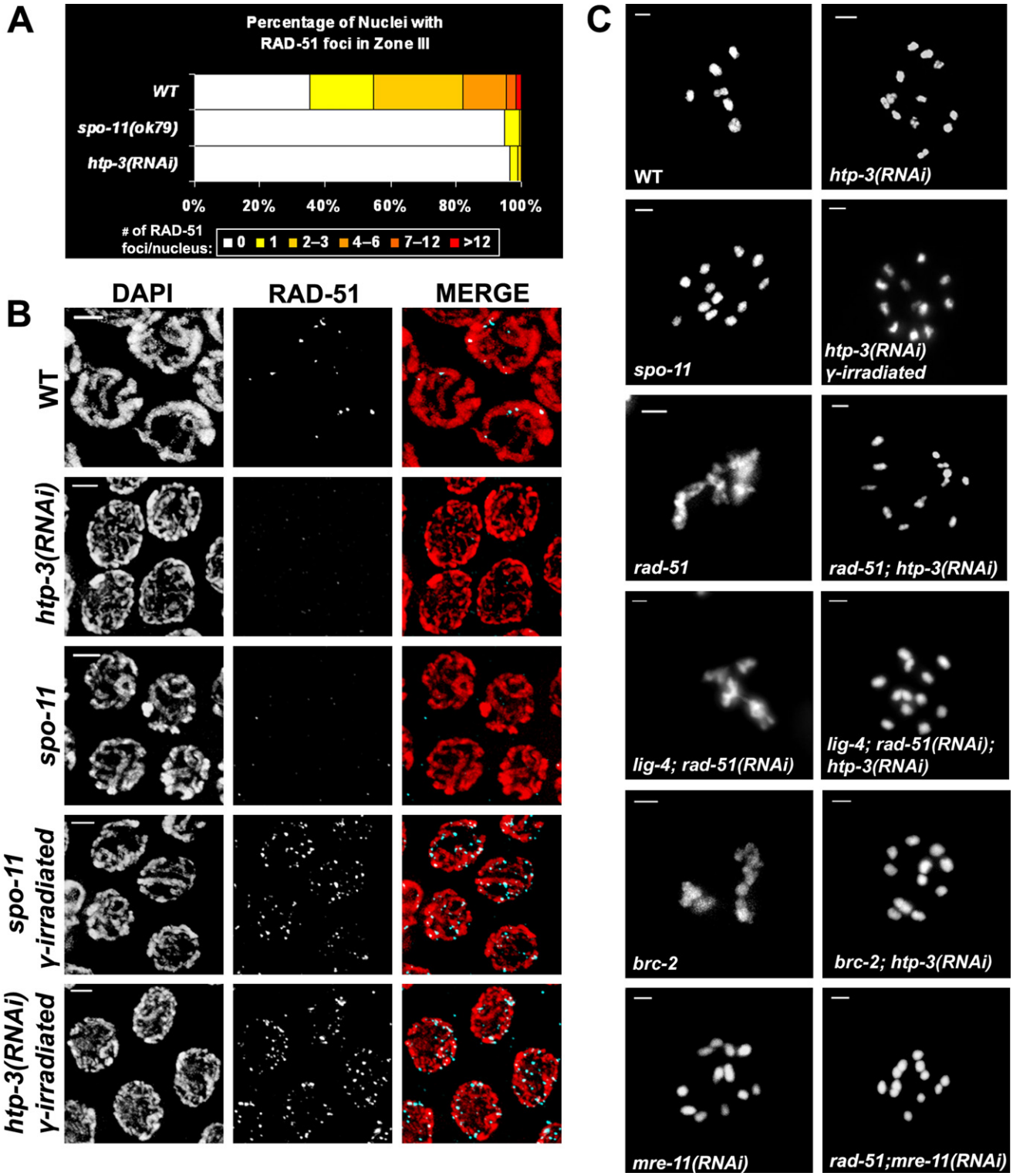

Figure 4. HTP-3 Is Required for DSB Formation in Meiotic Recombination

(A) Bar graph showing the percentage of individual nuclei from the early-pachytene region (zone III) containing either 0, 1, 2–3, 4–6, 7–12, or more than 12 RAD-51 foci in germlines of animals of the indicated genotypes. In wild-type germlines, the number of RAD-51 foci peaks in zone III, and in *spo-11* mutant germlines in which meiotic DSB formation is abrogated, only background levels can be detected. *htp-3(RNAi)* germline nuclei exhibited only background levels of RAD-51 foci not significantly different from those detected in *spo-11(ok79)* null mutants (probability of being different, $p = 0.0001$ by Mann-Whitney).

(B) Immunofluorescence micrographs showing defects in RAD-51 foci formation in zone III nuclei of Spo-11 mutants and *htp-3(RNAi)* germlines; introduction of artificial DSBs using γ-irradiation (Experimental Procedures) results in robust RAD-51 foci formation.

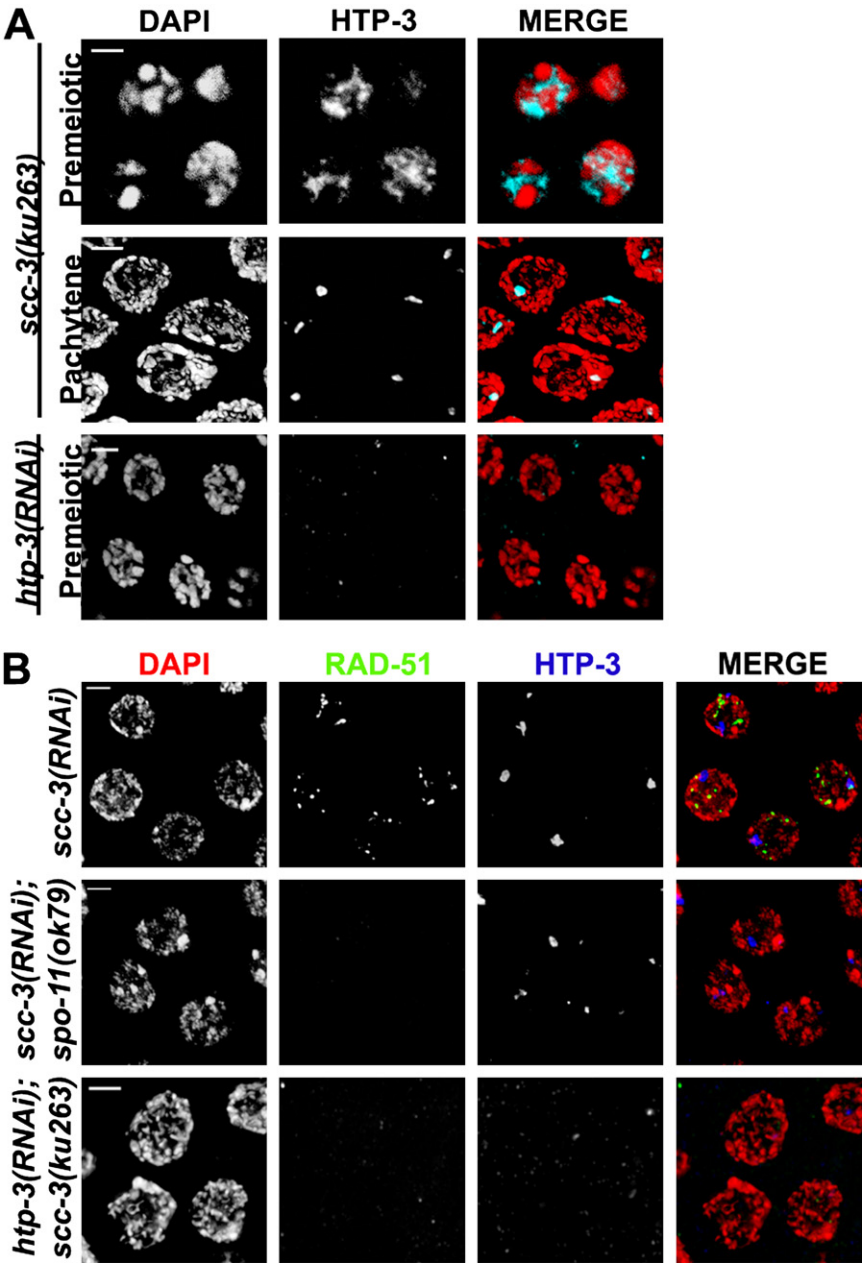

Figure 5. SCC-3-Dependent Localization of HTP-3 to Chromosome Axes Is Not Required for Recombination Initiation

(A) High-magnification images of premeiotic nuclei showing reduced HTP-3 localization to chromatin in *scc-3(ku263)* mutants and no detectable HTP-3 in *htp-3(RNAi)* germlines (compare to Figure 1). Pachytene-stage nuclei of *scc-3(ku263)* mutants show no detectable anti-HTP-3 signal at chromosome cores, and instead the protein localizes to one or two nuclear aggregates.

(B) Early-pachytene-stage nuclei of *scc-3(RNAi)* germlines showing high levels of RAD-51 foci and aggregation of HTP-3. RAD-51 foci formation is dependent on *spo-11* and on *htp-3*, indicating that the foci are early meiotic recombination intermediates and recombination initiation is dependent on *htp-3* in the absence of *scc-3*. Scale bars, 3 μm.

the proposal that the DSB machinery intimately interacts with axis components to propel the formation of meiotic DSBs to the context of chromosomal axes where their repair can be directed along an interhomolog pathway that generates crossovers (Zickler and Kleckner, 1999). To determine if HTP-3 localization to chromosome axes was essential for its function in meiotic recombination initiation, we examined RAD-51 focus formation in *scc-3*-depleted germlines in which HTP-3 fails to localize to chromosomes and instead aggregates in the nucleoplasm (Figure 5). We reasoned that if the localization of HTP-3 was required for its function in DSB formation, then RAD-51 foci formation in *scc-3*-depleted germlines should be similar to the levels observed in *htp-3(RNAi)* germlines; instead, large numbers of RAD-51 foci were observed in both *scc-3(RNAi)* and *scc-3(ku263)* mutant germlines (Table S1), consistent with previous reports of RAD-51 foci formation in *rec-8* cosuppressed germlines (Alpi et al., 2003). To confirm that these foci were the products of meiotic recombination initiation rather than RAD-51-marked DNA repair intermediates originating from the persistence of replication errors as a consequence of cohesion defects (Sonoda et al., 2001), we next stained for RAD-51 in *scc-3(RNAi); spo-11(ok59)* germlines (Figure 5B), in which programmed meiotic DSBs are eliminated due to the absence of SPO-11. We observed a reduction in RAD-51 foci in *scc-3(RNAi); spo-11(ok59)* germlines to levels comparable to those observed in *spo-11(ok79)* mutant germlines (>95% of the nuclei contain no RAD-51 foci; Table S1 and Figure 5A), indicating that the vast majority of foci detected in the *scc-3(ku263)* mutant were the result of meiotic recombination initiation. Next, we sought to confirm that the formation of meiotic DSBs in the absence of SCC-3 was also HTP-3 dependent, despite the fact that HTP-3 localizes to nuclear aggregates from the earliest

(C) DAPI-stained diakinesis nuclei of animals of the indicated genotype. In wild-type oocytes, six well-condensed bivalents are observed, while in *htp-3(RNAi)* (49/49 oocytes examined) and *spo-11* oocytes, 12 univalents are observed, indicating a failure in chiasma formation. In γ-irradiated germlines of *htp-3(RNAi)* animals, 12 well-formed univalents appear at diakinesis, indicating that DSB repair can proceed in the absence of HTP-3. *rad-51(lg8701)* and *brc-2 (tm1086)* mutant oocytes exhibit a DSB-dependent defect in chromatin condensation; this phenotype is rescued by *htp-3(RNAi)*, independent of the activity of the central NHEJ ligase *lig-4,* and by *mre-11(RNAi)*, resulting in 12 well-formed univalents. Scale bars, 2 μm.

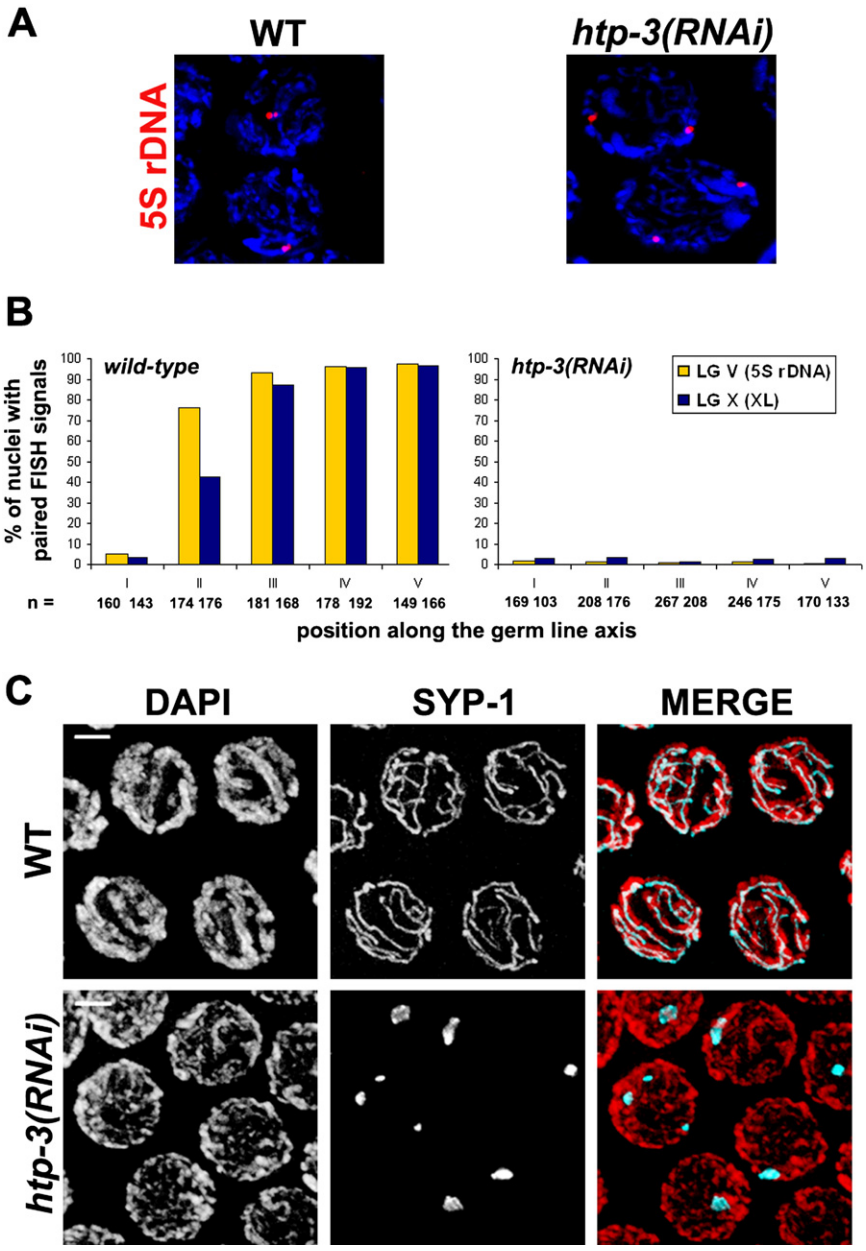

Figure 6. HTP-3 Is Required for Homolog Alignment and Synapsis

Hermaphrodite gonads were divided into five equivalently sized intervals along the proximal-distal axis (45–50 μm each) corresponding to the following stages: prmeiotic zone (I), leptotene-zygotene (II), and early-, mid-, and late-pachytene (III–V). A single-copy probe was used to monitor pairing of loci on chromosome X left (LG XL), and a probe targeting the 5S rDNA locus located approximately 15% of the chromosome length from the right end of chromosome V (5S rDNA).

(A) Immunofluorescence micrographs showing paired and unpaired FISH signals in wild-type and *htp-3(RNAi)* mid-pachytene-stage nuclei, respectively.

(B) Histograms showing pairing levels for the indicated probes in each genotype. Pairing levels in *htp-3(RNAi)* did not rise significantly above background levels in the premeiotic zone for either probe (probability of being different, p = 0.0001 by Fisher's Exact Test). For each zone, the following numbers of nuclei were scored: wild-type-5S probe (160, 174, 181, 178, 149), wild-type-X probe (143, 176, 168, 192, 166), *htp-3(RNAi)*-5S probe (169, 208, 267, 246, 170), *htp-3(RNAi)*-X probe (103, 176, 208, 175, 133).

(C) In wild-type mid-pachytene-stage germline nuclei, DAPI-stained chromosomes are organized in parallel tracks characteristic of synapsed chromosomes. The central element component SYP-1 localizes to long continuous bands between homologous chromosomes. In the mid-pachytene interval of *htp-3(RNAi)* germlines, pachytene nuclei are disorganized and lack the side-by-side arrangement of DAPI-stained chromosomes, and SYP-1 fails to localize and instead forms nuclear aggregates, indicating a failure in synapsis. Scale bars, 2 μm.

stages of meiotic prophase; no RAD-51 foci could be detected above background levels in *spo-11(ok79); scc-3(RNAi)* or *htp-3(RNAi);scc-3(ku263)* mutant germlines (Figure 5B), and quantification of these foci detected no statistical difference between the two genotypes (p = 0.38 by two-tailed Mann-Whitney Test, C.I. 95%). We next investigated if MRE-11 colocalized into the nuclear aggregates of HTP-3 observed in *scc-3* mutants; however, no overt localization of MRE-11 into the aggregates could be detected (data not shown). Consequently, MRE-11 may still interact with the residual chromatin-associated pool of HTP-3 detectable in premeiotic nuclei to mediate DSB formation in *scc-3* mutants, or HTP-3 may have an MRE-11-independent function in the process. Nevertheless, our results demonstrate that meiotic DSB formation requires HTP-3 in the absence of SCC-3 (and cohesin; Wang et al., 2003) and that the localization of HTP-3 to meiotic chromosome axes is not required for its function during recombination initiation.

HTP-3 Is Required for Homolog Alignment and Synapsis

HIM-3 is a *C. elegans* meiosis-specific noncohesin component of chromosome axes that we have shown to be required for both initial homolog alignment and for synapsis (Zetka et al., 1999; Couteau et al., 2004). Given that HTP-3 complexes contain HIM-3 and that HTP-3 is required for localization of HIM-3 to chromosome axes, the loss of HTP-3 would be predicted to result in severe meiotic defects independent of its role in meiotic DSB formation. To investigate the consequences of HTP-3 loss on these processes, chromosome behavior was examined in *htp-3(RNAi)* hermaphrodites. A time course analysis of pairing levels in *htp-3(RNAi)* hermaphrodites using fluorescence in situ hybridization (FISH) to several chromosomal loci was performed (Figures 6A and 6B); paired FISH signals in *htp-3(RNAi)* germlines were never observed above the background level detected in the premeiotic region, indicating that HTP-3 was required for the establishment of initial homolog alignment. Furthermore, the DAPI-stained

chromosomes of nuclei in the pachytene region of the germline failed to adopt the equidistant, side-by-side alignment characteristic of synapsed chromosomes (Figure 6C; MacQueen et al., 2002), and localization of SYP-1, a central region SC component required for synapsis SYP-1, was limited to one or a few small nuclear aggregates in the pachytene region (Figure 6C), reminiscent of the localization of SYP-1 in *him-3* null mutants in which chromosomes fail to synapse (Couteau et al., 2004).

DISCUSSION

HTP-3 Links Meiotic DSB Formation with Chromosome Pairing, Synapsis, and Interhomolog Recombination

Our analysis has identified HTP-3 as a key meiotic regulator that is required for the fundamental meiotic processes of DSB formation during meiotic recombination initiation, homolog alignment, and synapsis. In the absence of HTP-3, chromosomes fail to attain early alignment and synapsis as evidenced by (1) the lack of paired FISH signals throughout meiotic prophase, (2) the lack of parallel DAPI-stained tracts in pachytene nuclei, (3) the failure to recruit SC components like SYP-1 to chromosomes and the localization of SYP-1 to the nuclear aggregates observed in other synapsis-defective mutants, and (4) the failure to form chiasmata at diakinesis (Colaiácovo et al., 2003; Couteau et al., 2004). These defects are strikingly similar to those reported for mutants in *him-3* (Couteau et al., 2004), and in fact HTP-3 interacts with HIM-3 in yeast two-hybrid screens (data not shown), HTP-3-immunoprecipitated complexes contain HIM-3, and HTP-3 localization to chromosome axes is required for subsequent association of HIM-3, indicating that the two proteins physically interact. While the possibility that HTP-3 has independent functions in homolog alignment, synapsis, and chiasma formation remains, the simplest interpretation is that the role of HTP-3 in these processes is molecularly effected through HIM-3 recruitment to meiotic chromosome axes.

In stark contrast to *him-3* null mutants in which recombination is initiated on time and at wild-type levels (Couteau et al., 2004), no RAD-51- or RPA-1-marked early recombination intermediates could be detected in the absence of HTP-3. Since RAD-51 could be recruited to artificially provided DSBs in irradiated *htp-3(RNAi)* germlines and no chromosome fragmentation or chromatin condensation defects were observed at diakinesis, we conclude that DSBs can be efficiently processed and repaired using HR in the absence of HTP-3, similar to other synapsis-defective mutants where homologous chromosomes are unavailable as templates for repair (Colaiácovo et al., 2003; Couteau et al., 2004; Smolikov et al., 2007). The failure to detect early RAD-51-marked HR recombination intermediates in *htp-3(RNAi)* germlines could be explained by the repair of meiotic DSBs via an inappropriate non-HR pathway, or by the failure to form DSBs per se. However, our observations argue for the latter interpretation since the depletion of *htp-3* by RNAi rescues the DSB-dependent chromosome aggregation defects observed at diakinesis in both *rad-51* (required for HR) and *brc-2* mutants (required for HR and for RAD-51-independent BRC-2-dependent DSB repair activity; Martin et al., 2005). This rescue occurs independently of the NHEJ core component *lig-4*, indicating that it does not require the activity of any known DSB repair pathway. Taken together, our study provides multiple lines of evidence that collectively suggest that HTP-3 is essential for meiotic DSB formation.

Our biochemical analyses reveal that HTP-3 forms a complex with MRE-11 and RAD-50 in vivo, and several lines of evidence point to a conserved role for MRE-11 in meiotic DSB formation. Unlike *rad-51* mutants, the diakinesis univalents observed in *mre-11* mutants are well condensed, despite their inability to repair artificially provided DSBs, consistent with the interpretation that meiotic DSBs fail to form in *mre-11* mutants (Chin and Villeneuve, 2001). Furthermore, depletion of *mre-11* rescues the DSB-dependent chromosome defects in the diakinesis nuclei of *rad-51* mutants. Because MRE-11 is unstable in the absence of RAD-50 (Figure 6), the evidence collectively suggests that MRE-11 and RAD-50 form a conserved complex (similar to the MRX complex)—possibly including the putative nematode Xrs2 homolog XNP-1 (Garcia-Muse and Boulton, 2007)—that is required for both the formation and the processing (5′ to 3′ resection) of the regulated DSBs that initiate meiotic recombination.

Given that HTP-3 forms a complex with MRE-11/RAD-50, the simplest explanation for the requirement for HTP-3 in meiotic DSB formation is at the level of its interaction with MRE-11 and RAD-50. HTP-3 does not appear to be required for bulk stabilization or localization of the MRE-11/RAD-50 complex to chromosomes since WT-like levels of MRE-11 foci form in meiotic *htp-3(RNAi)* nuclei, and a large fraction colocalize with chromatin. A similar pattern of localization is also observed in *spo-11* mutants (data not shown), indicating that in *C. elegans*, as in budding yeast, SPO-11 is not required for bulk MRE-11 localization. These results are consistent with the emerging model that the DSB complex is composed of subgroups of interacting proteins that successively cooperate to facilitate SPO-11-dependent cleavage, rather than a preassembled holoenzyme stoichiometrically composed of subunits required for DSB formation (Maleki et al., 2007). Consequently, the HTP-3/MRE-11/RAD-50 complex may represent a chromosome-associated pre-DSB subcomplex that cooperates with other DSB subgroups to facilitate SPO-11-mediated meiotic DSB catalysis; however, given our inability to detect colocalization of HTP-3 and MRE-11, it is unknown whether the interaction between HTP-3 and MRE-11 is direct or involves other bridging factors, and we cannot exclude the possibility that HTP-3 has an MRE-11-independent function in DSB formation.

We observed that HTP-3 is required for recombination initiation in *scc-3* mutants and that the mislocalization of HTP-3 from chromosome axes from the earliest stages of meiotic prophase does not block meiotic recombination initiation, suggesting that the axis-associated population is dispensable for meiotic DSB formation. Previous studies in budding yeast have shown that mutants in meiotic axis components show severe defects in DSB formation (reviewed by Keeney, 2001); reduced steady-state levels of DSBs are observed in mutants of Red1p, and even more drastic reductions are observed in mutants of Hop1p (Mao-Draayer et al., 1996; Xu et al., 1997; Woltering et al., 2000). However, evidence exists that the function of Hop1p in establishing appropriate DSB levels occurs outside of its bulk localization to chromosome axes; although axis association of Hop1p is dependent on prior localization of Red1p, *HOP1* mutants are epistatic to *RED1* mutants for recombination defects, revealing a Red1p-independent and axis-association-independent requirement for

Hop1p (Rockmill and Roeder, 1990). Similarly, we propose that it is the chromatin-associated pool of HTP-3 observed in WT and Scc-3 nuclei in premeiotic S phase that is required for this function.

The shift of HTP-3 from chromatin to assembling chromosomal axes upon entry into meiotic prophase and the subsequent recruitment of HIM-3 has functional implications for the recombination pathway beyond recombination initiation. In mutants of the SC components *syp-1* (MacQueen et al., 2002) and *syp-2* (Colaiácovo et al., 2003), chromosome axes assemble normally and recruit HIM-3 but fail to synapse. Nevertheless, recombination is initiated at wild-type levels, but RAD-51-marked recombination intermediates accumulate and persist into inappropriately late stages and trigger the pachytene DNA damage checkpoint, revealing a barrier to using the sister chromatid as a repair template during early- and mid-pachytene (Colaiácovo et al., 2003). In contrast, the wild-type levels of RAD-51 intermediates that form in *him-3* null mutants disappear with wild-type kinetics, despite the fact that the chromosomes fail to synapse and homologous partners are also spatially unavailable for exchange (Couteau et al., 2004). These observations suggest HIM-3 is a component of the BSCE that promotes the use of the homolog as repair template and crossover formation (Couteau et al., 2004). Thus the functions of HTP-3 in recombination are multifold—the protein is required to generate the initiating DSB events and then, following its localization to meiotic chromosome axes, promotes interhomolog repair of the DSB and maturation into chiasmata via HIM-3 recruitment and HIM-3-mediated homolog alignment, BSCE, and synapsis.

EXPERIMENTAL PROCEDURES

Genetics

Bristol strain N2 was used as the wild-type control and all experiments were conducted at 20°C under standard conditions (Brenner, 1974). Mutant strains were obtained from the *Caenorhabditis* Genetics Center (University of Minnesota, St. Paul) and *C. elegans* Gene Knockout Consortium. The following mutations and rearrangements were used (LG, linkage group): LG III: *brc-2(tm1086), lig-4(ok716)*; LG IV: *him-3(gk149), spo-11(ok79), rad-51(lg8701)*; LG V: *scc-3(ku263), mre-11(ok179)*.

Production and Testing of Antibodies

A PCR fragment encoding amino acids 414 to 607 of HTP-3 was amplified from cDNA yk184d3 using the following forward and reverse primers, respectively: AAGGATCCCTTGTACCTCCAGTTGAAGTCGATG and TTCTCGAGAGCTGC TTCTTCATGCTGCTCGGTG. The fragment was cloned in frame with the His-tag of the pHEX cloning vector (gift from Scott Page) using BamHI and XhoI restriction sites. Recombinant protein was expressed and purified using Ni-NTA technology according to manufacturer's protocol (QIAGEN). Rabbits and guinea pigs were immunized according to standard protocols (Cocalico Biologicals, Inc.). HTP-3 and HIM-3 antibodies were purified by immunoaffinity chromatography with activated immunoaffinity supports (Affi-Gel 10/15, Bio-rad), according to manufacturers' instructions. The specificity of HTP-3 antibodies was demonstrated by the following criteria: no signal could be detected using preimmune sera; identical staining patterns were observed with both rabbit and guinea pig polyclonal sera; no HTP-3 staining could be detected in *htp-3(RNAi)* germlines. To generate an anti-MRE-11 antibody, a C-terminal synthetic peptide (CKVVSTRQIDSDGFEIINDSP) was generated (Peptide Synthesis Laboratory, Cancer Research UK). Rabbits were immunized (Harlan Sera Labs, Loughborough, UK) with 1 mg of the peptide coupled to activated keyhole limpet hemocyanin (Pierce, Rockford, IL). Antibodies were affinity purified as described previously, dialyzed overnight against 20 mM Tris-acetate (pH 8.0), 0.2 M potassium acetate, 10% glycerol, 1 mM EDTA, and 0.5 mM dithiothreitol (Martin et al., 2005). The purified antibodies were then tested in N2 and *mre-11(ok179)* worms before and after treatment with either 150 Gy of ionizing radiation, 180 mM cisplatin, or 200 mM nitrogen mustard. The mitotic signal observed in N2 worms is damage specific and absent in *mre-11* mutants. The meiotic signal is not specific to damage and is absent in *mre-11* mutants.

Cytological Methods

DAPI staining, immunostaining and imaging, and FISH analysis was performed as described in Couteau et al. (2004), using identical probes specific for the 5S rDNA locus (chromosome V) and left end of the X chromosome. Images presented are high-magnification (100x) projections consisting of 20–30 0.2 μM slices encompassing entire nuclei. Primary antibodies were used at the following dilutions: rabbit anti-HTP-3 (1:200), guinea pig anti-HTP-3 (1:200), anti-HIM-3 (1:200) (Zetka et al., 1999), anti-SYP-1 (1:100) (MacQueen et al., 2002), anti-Ce-RAD-51 (1:100) (Rinaldo et al., 2002), anti-RPA-1 (1:100) (Martin et al., 2005), and anti-MRE-11 (1:100). The following secondary antibodies were used at a dilution of 1:500: Alexa Fluor 488 anti-rabbit, Alexa Fluor 555 anti-guinea pig (Molecular Probes).

RNA Interference

The existing mutation of *htp-3, gk26*, is a deletion allele tightly linked to a complex rearrangement that includes a wild-type copy of the gene; consequently, the strain has no phenotype (F. Couteau and M. Zetka, unpublished data). RNA interference experiments were performed as described previously (Fire et al., 1998). Three other paralogs of *htp-3* (*him-3*, *htp-1*, and *htp-2*) have been identified in *C. elegans* but were not expected to be affected by interference with *htp-3* RNA because of limited sequence similarity. Staged adult hermaphrodites (20–22 hr post-L4) were injected with ~500 ng/μl *htp-3* dsRNA in the pachytene region of each gonad arm and transferred to fresh plates every ~15 hr. At 70 hr postinjection, the worms were dissected, fixed, and stained as described above. Bacteria-mediated RNAi was performed under the conditions described in Fraser et al. (2000) using *scc-3* (F18E2.3) or *spo-11* (T05E11.4) dsRNA-expressing bacteria (MRC Geneservice).

Immunoprecipitation

Adult N2 worms were frozen and ground, and the resulting powder was melted on ice in homogenization buffer (50 mM HEPES-KOH [pH 7.6], 1 mM EDTA, 140 mM KCl, 0.5% NP-40, 10% glycerol, 5 mM 2-Mercaptoethanol, and protease inhibitor cocktail [Complete Mini, Roche Diagnostics]) and centrifuged for 10 min at 16,000 g. The supernatant was used for immunoprecipitation according to Chu et al. (2002). For the control IP, the antibody was blocked by preincubation with a 50–100-fold excess of antigen at 20°C for 1 hr.

γ-Irradiation Experiments

Worms injected with *htp-3* dsRNA were exposed to 5000 rads of γ-irradiation 70 hr postinjection and processed for immunofluorescence 4 hr later.

Statistics

Significance of pairing levels was tested by Fisher's Exact Test (two-tailed p value and 95% confidence intervals [C.I.]). RAD-51 foci distribution was compared by a Mann-Whitney test (two-tailed p, 95% C.I.), where positive and negative nuclei for RAD-51 staining were taken into consideration. All calculations were performed with InStat3 software (Graphpad).

Supplemental Data

Supplemental Data include three figures and one table and can be found with this article online at http://www.developmentalcell.com/cgi/content/full/14/2/263/DC1/.

ACKNOWLEDGMENTS

The authors would like to thank James Rankin, Patrick Allard, and the members of the laboratory of Richard Roy for technical assistance and helpful discussions; the *Caenorhabditis* Genetics Center, International *C. elegans* Gene Knockout Consortium, Yuji Kohara, and Sanger Center for strains and clones; and Anne Villeneuve, Adriana LaVolpe, and Anton Gartner for antibodies. J.D.W. and S.J.B. are funded by Cancer Research UK. This work was

supported by a CIHR Postdoctoral Fellowship to S.K. and by grants from the Canadian Institutes of Health Research (CIHR) and the National Cancer Institute of Canada (NCIC) to M.C.Z.

Received: July 30, 2007
Revised: October 18, 2007
Accepted: November 17, 2007
Published: February 11, 2008

REFERENCES

Alpi, A., Pasierbek, P., Gartner, A., and Loidl, J. (2003). Genetic and cytological characterization of the recombination protein rad-51 in *Caenorhabditis elegans.* Chromosoma *112*, 6–16.

Brenner, S. (1974). The genetics of *Caenorhabditis elegans.* Genetics *77*, 71–94.

Chan, R.C., Chan, A., Jeon, M., Wu, T.F., Pasqualone, D., Rougvie, A.E., and Meyer, B.J. (2003). Chromosome cohesion is regulated by a clock gene paralogue TIM-1. Nature *423*, 1002–1009.

Chin, G.M., and Villeneuve, A.M. (2001). *C. elegans mre-11* is required for meiotic recombination and DNA repair but is dispensable for the meiotic G_2 DNA damage checkpoint. Genes Dev. *15*, 522–534.

Chu, D.S., Dawes, H.E., Leib, J.D., Chan, R.C., Kuo, A.F., and Meyer, B.J. (2002). A molecular link between gene-specific and chromosome-wide transcriptional repression. Genes Dev. *16*, 796–805.

Clejan, I., Boerckel, J., and Ahmed, S. (2006). Developmental modulation of nonhomologous end joining in *Caenorhabditis elegans.* Genetics *173*, 1301–1317.

Colaiácovo, M.P., MacQueen, A.J., Martinez-Perez, E., McDonald, K., Adamo, A., La Volpe, A., and Villeneuve, A.M. (2003). Synaptonemal complex assembly in *C. elegans* is dispensable for loading strand-exchange proteins but critical for proper completion of recombination. Dev. Cell *5*, 463–474.

Couteau, F., and Zetka, M. (2005). HTP-1 coordinates synaptonemal complex assembly with homolog alignment during meiosis in *C. elegans.* Genes Dev. *19*, 2744–2756.

Couteau, F., Nabeshima, K., Villeneuve, A.M., and Zetka, M. (2004). A component of *C. elegans* meiotic chromosome axes at the interface of homolog alignment, synapsis, nuclear reorganization, and recombination. Curr. Biol. *14*, 585–592.

Dernburg, A.F., McDonald, J., Moulder, G., Barstead, R., Dresser, M., and Villeneuve, A.M. (1998). Meiotic recombination in *C. elegans* initiates by a conserved mechanism and is dispensable for homologous chromosome synapsis. Cell *94*, 387–398.

Fire, A., Xu, S., Montgomery, M.K., Kostas, S.A., Driver, S.E., and Mello, C.C. (1998). Potent and specific genetic interference by double-stranded RNA in *Caenorhabditis elegans.* Nature *391*, 806–811.

Fraser, A.G., Kamath, R.S., Zipperlen, P., Martinez-Campos, M., Sohrmann, M., and Ahringer, J.A. (2000). Functional genomic analysis of *C. elegans* chromosome I by systemic RNA interference. Nature *408*, 325–330.

Garcia-Muse, T., and Boulton, S.J. (2007). Meiotic recombination in *Caenorhabditis elegans*. Chromosome Res. *15*, 607–621.

Henderson, K.A., and Keeney, S. (2005). Synaptonemal complex formation: where does it start? Bioessays *27*, 995–998.

Henderson, K.A., Kee, K., Maleki, S., Santini, P., and Keeney, S. (2006). Cyclin-dependent kinase directly regulates initiation of meiotic recombination. Cell *125*, 1321–1332.

Keeney, S. (2001). Mechanism and control of meiotic recombination initiation. Curr. Top. Dev. Biol. *52*, 1–53.

Kelly, K.O., Dernburg, A.F., Stanfield, G.M., and Villeneuve, A.M. (2000). *Caenorhabditis elegans msh-5* is required for both normal and radiation-induced meiotic crossing over but not for completion of meiosis. Genetics *156*, 617–630.

Kleckner, N. (2006). Chiasma formation: chromatin/axis interplay and the role(s) of the synaptonemal complex. Chromosoma *115*, 175–194.

MacQueen, A.J., Colaiácovo, M.P., McDonald, K., and Villeneuve, A.M. (2002). Synapsis-dependent and –independent mechanisms stabilize homolog pairing during meiotic prophase in *C. elegans.* Genes Dev. *16*, 2428–2442.

MacQueen, A.J., Phillips, C.M., Bhalla, N., Weiser, P., Villeneuve, A.M., and Dernburg, A.F. (2005). Chromosome sites play dual roles to establish homologous synapsis during meiosis in *C. elegans.* Cell *123*, 1037–1050.

McKim, K.S., Green-Marroquin, B.L., Sekelsky, J.J., Chin, G., Steinberg, C., Khodosh, R., and Hawley, R.S. (1998). Meiotic synapsis in the absence of recombination. Science *279*, 876–878.

Maleki, S., Neale, M.J., Arora, C., Henderson, K.A., and Keeney, S. (2007). Interactions between Mei4, Rec114, and other proteins required for meiotic DNA double-strand break formation in *Saccharomyces cerevisiae.* Chromosoma *116*, 471–486.

Mao-Draayer, Y., Galbraith, A.M., Pittman, D.L., Cool, M., and Malone, R.E. (1996). Analysis of recombination pathways in the yeast *Saccharomyces cerevisiae.* Genetics *144*, 71–86.

Martin, J.S., Winkelmann, N., Petalcorin, M.I.R., McIlwraith, M.J., and Boulton, S.J. (2005). RAD-51-dependent and –independent roles of a *Caenorhabditis elegans* BRCA2-related protein during DNA double-strand break repair. Mol. Cell. Biol. *25*, 3127–3139.

Martinez-Perez, E., and Villeneuve, A.M. (2005). HTP-1-dependent constraints coordinate homolog pairing and synapsis and promote chiasma formation during *C. elegans* meiosis. Genes Dev. *19*, 2727–2743.

Murakami, H., Borde, V., Shibata, T., Lichten, M., and Ohta, K. (2003). Correlation between premeiotic DNA replication and chromatin transition at yeast recombination initiation sites. Nucleic Acids Res. *31*, 4085–4090.

Neale, M.J., and Keeney, S. (2006). Clarifying the mechanics of DNA strand exchange in meiotic recombination. Nature *442*, 153–158.

Neale, M.J., Pan, J., and Keeney, S. (2005). Endonucleolytic processing of covalent protein-linked DNA double-strand breaks. Nature *436*, 1053–1057.

Nasmyth, K., and Haering, C.H. (2005). The structure and function of SMC and kleisin complexes. Annu. Rev. Biochem. *74*, 595–648.

Niu, H., Wan, L., Baumgartner, B., Schaefer, D., Loidl, J., and Hollingsworth, N.M. (2005). Partner choice during meiosis is regulated by Hop1-promoted dimerization of Mek1. Mol. Biol. Cell *16*, 5804–5818.

Pasierbek, P., Jantsch, M., Melcher, M., Schleiffer, A., Schweizer, D., and Loidl, J. (2001). A *Caenorhabditis elegans* cohesion protein with functions in meiotic chromosome pairing and disjunction. Genes Dev. *15*, 1349–1360.

Pasierbek, P., Fodermayr, M., Jantsch, V., Jantsch, M., Schweizer, D., and Loidl, J. (2003). The *Caenorhabditis elegans* SCC-3 homologue is required for meiotic synapsis and for proper chromosome disjunction in mitosis and meiosis. Exp. Cell Res. *289*, 245–255.

Peoples, T.L., Dean, E., Gonzalez, O., Lambourne, L., and Burgess, S.M. (2002). Close, stable homolog juxtaposition during meiosis in budding yeast is dependent on meiotic recombination, occurs independently of synapsis, and is distinct from DSB-dependent pairing contacts. Genes Dev. *16*, 1682–1695.

Reddy, K.C., and Villeneuve, A.M. (2004). *C. elegans* HIM-17 links chromatin modification and competence for initiation of meiotic recombination. Cell *118*, 439–452.

Reinke, V., Gil, I.S., Ward, S., and Kazmer, K. (2004). Genome-wide germline-enriched and sex-biased expression profiles in *Caenorhabditis elegans.* Development *131*, 311–323.

Rinaldo, C., Bazzicalupo, P., Ederle, S., Hilliard, M., and La Volpe, A. (2002). Roles for *Caenorhabditis elegans rad-51* in meiosis and in resistance to ionizing radiation during development. Genetics *160*, 471–479.

Rockmill, B., and Roeder, G.S. (1990). Meioisis in asynaptic yeast. Genetics *126*, 563–574.

Smolikov, S., Eizinger, A., Hurlburt, A., Rogers, E., Villeneuve, A.M., and Colaiácovo, M.P. (2007). Synapsis-defective mutants reveal a correlation between chromosome conformation and the mode of double-strand break repair during *Caenorhabditis elegans* meiosis. Genetics *176*, 2027–2033.

Sonoda, E., Matsusaka, T., Morrison, C., Vagnarelli, P., Hoshi, O., Ushiki, T., Nojima, K., Fukagawa, T., Waizenegger, I.C., Peters, J.M., et al. (2001).

Scc1/Rad21/Mcd1 is required for sister chromatid cohesion and kinetochore function in vertebrate cells. Dev. Cell *1*, 759–770.

Takanami, T., Mori, A., Takahashi, H., Horiuchi, S., and Higashitani, A. (2003). *Caenorhabditis elegnas Ce-rdh-1/rad-51* functions after double-strand break formation of meiotic recombination. Chromosome Res. *11*, 125–135.

Tessé, S., Storlazzi, A., Kleckner, N., Gagano, S., and Zickler, D. (2003). Localization and roles of Ski8p protein in Sordaria meiosis and delineation of three mechanistically distinct steps of meiotic homolog juxtaposition. Proc. Natl. Acad. Sci. USA *100*, 12865–12870.

Wang, F., Yoder, J., Antoshechkin, I., and Han, M. (2003). *Caenorhabditis elegans* EVL-14/PDS-5 and SCC-3 are essential for sister chromatid cohesion in meiosis and mitosis. Mol. Cell. Biol. *23*, 7698–7707.

Woltering, D., Baumgartner, B., Bagchi, S., Larkin, B., Loidl, J., de los Santos, T., and Hollingsworth, N.M. (2000). Meiotic segregation, synapsis, and recombination checkpoint functions require physical interaction between the chromosomal proteins Red1p and Hop1p. Mol. Cell. Biol. *20*, 6646–6658.

Xu, L., Weiner, B.M., and Kleckner, N. (1997). Meiotic cells monitor the status of the interhomolog recombination complex. Genes Dev. *11*, 106–118.

Zetka, M.C., Kawasaki, I., Strome, S., and Muller, F. (1999). Synapsis and chiasma formation in *Caenorhabditis elegans* require HIM-3, a meiotic chromosome core component that functions in chromosome segregation. Genes Dev. *13*, 2258–2270.

Zickler, D. (2006). From early homologue recognition to synaptonemal complex formation. Chromosoma *115*, 158–174.

Zickler, D., and Kleckner, N. (1999). Meiotic chromosomes: Integrating structure and function. Annu. Rev. Genet. *33*, 603–754.